PHOTONICS Research

Multiparticle resonant optical sorting using a topological photonic structure

Bojian Shi,[1] Yongyin Cao,[1] Tongtong Zhu,[2] Hang Li,[1] Yanxia Zhang,[1] Rui Feng,[1] Fangkui Sun,[1] and Weiqiang Ding[1,3,*]

[1]Institute of Advanced Photonics, School of Physics, Harbin Institute of Technology, Harbin 150001, China
[2]School of Optoelectronic Engineering and Instrumentation Science, Dalian University of Technology, Dalian 116024, China
[3]Collaborative Innovation Center of Extreme Optics, Shanxi University, Taiyuan 030006, China
*Corresponding author: wqding@hit.edu.cn

Received 26 August 2021; revised 7 November 2021; accepted 18 November 2021; posted 18 November 2021 (Doc. ID 441644); published 7 January 2022

Resonance between light and object is highly desired in optical manipulation because the optical forces reach maximum values in this case. However, in traditional waveguide structures, the resonant interaction also greatly perturbs the incident field and weakens or completely destroys the manipulation on the subsequent particles. In order to avoid this dilemma, we propose to perform optical manipulation in a topological photonic structure. Owing to the topological protection, the light mode can almost keep its original form when an object is being manipulated. Therefore, resonant optical sorting can be achieved in a multiple and high throughput manner. The mechanism and results presented here pave the way for efficient on-chip optical sorting for biophysical and biochemical analysis.

https://doi.org/10.1364/PRJ.441644

1. INTRODUCTION

Recently, optical sorting based on an optical waveguide has demonstrated tremendous potential for applications in pharmacies [1], diagnosis of cancer cells [2,3], purification of water [4], etc., due to the advantages of scalability, long-range manipulation, high throughput, high capacity, and easy integration with lab-on-a-chip systems [2,5–9]. In these manipulations, an optical force can sustainedly propel a variety of microparticles such as dielectric microparticles [10], metallic nanoparticles [11,12], and cells [13], and sort these microparticles [14].

In order to make the optical sorting more efficient, it is better to make the object resonant with the light source [15–17]. It is reported that the optical force on microparticles under resonant conditions can approach nearly the limit of totally absorbing particles [15]. And the propulsion velocities of the microparticles can accelerate 1 order faster than the previous observations in nonresonance [5,13,18–21]. Unfortunately, however, the resonant optical sorting with enhanced optical forces is not suitable for multiparticle optical sorting in waveguide structures. For the widely used optical sorting using a dielectric optical waveguide, as shown in Fig. 1(a), the second particle cannot be manipulated efficiently anymore (i.e., F_{z2} will be far less than F_{z1}), because the guiding mode is coupled efficiently with the first one at the peaks shown in Fig. 1(c) and also perturbed seriously by the particle. As a result, only a small fraction of the light acts on the second particle, as shown in Fig. 1(b). Therefore, the optical force on the second sphere becomes very small, as shown in Fig. 1(c). Here, it is noted that the repulsive behavior of the optical force at resonance is due to the asymmetric mode distribution [22–24]. Actually, when the coupling efficiency between the waveguide and the first particle approaches 1, the transmittance may drop to near zero, which results in the failure of sorting of subsequent particles.

In order to improve the transmittance and reduce the mode disturbance, the edge-to-edge distance d [see Fig. 1(b)] between the particle and the waveguide is a crucial parameter. For multiparticle optical sorting, the ratio of the optical forces on the second particle to that on the first particle, i.e., F_2/F_1, is introduced to quantitatively measure the influence of the first particle on the second one. The smaller F_2/F_1 is, the greater influence of the first particle on the second one. Figure 1(d) shows the resonance force F_z (upper part) and F_{z2}/F_{z1} (lower part) for different distances d. When d is less than some critical value d_c ($d_c = 120$ nm for current parameters), F_z increases with d, while the ratio F_{z2}/F_{z1} decreases rapidly. When $d > d_c$, the optical forces on the particles are weakened gradually, although F_{z2}/F_{z1} increases slightly. In any case, the optical force on the second particle is much smaller than the maximum resonant force on the first particle. Owing to these facts, only a single particle can be manipulated efficiently, and multiple particle sorting seems impossible.

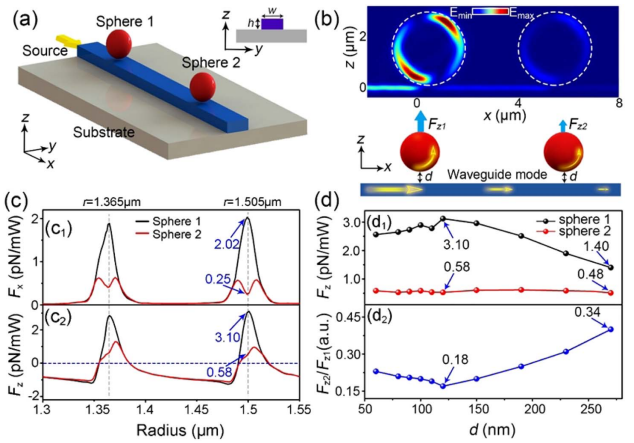

Fig. 1. Schematic and performances of resonant optical manipulation using the traditional optical waveguide. (a) Schematic of optical manipulation based on a strip waveguide (GaAs). The parameters are $w = 1$ μm, $h = 0.2$ μm, and light source frequency of $f = 315$ THz. The two red spheres are to be manipulated in water. (b) The resonance of sphere 1 with the incident light generates a large repulsive force F_{z1}. The repulsive force F_{z2} on sphere 2, however, is 1 order smaller than F_{z1}, because the guiding mode is greatly scattered by sphere 1. (c) Optical forces of F_x (upper part) and F_z (lower part) as a function of particle radius r. (d) Resonance force F_z on the two particles (upper part) and the ratio F_{z2}/F_{z1} (lower part) as a function of the distance d between the waveguide and the particle.

In order to overcome this drawback, in this paper, we propose to perform optical sorting using a topological photonic crystal (PC) structure, which supports a topology-protected guiding mode [25,26], as shown in Fig. 2(a). Because of the topology-protected feature, the propagation of the light field is immune to the local disorders, including the objects to be sorted [Fig. 2(b)]. Thus, the optical sorting mechanism proposed here is extremely efficient and has a high throughput for multiparticle optical sorting.

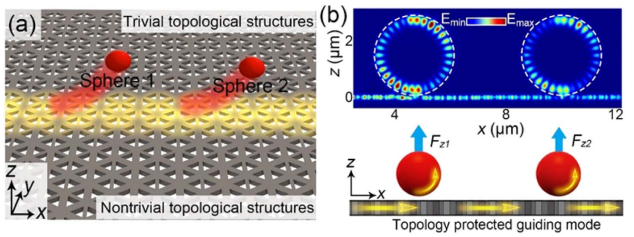

Fig. 2. Schematic of resonant optical manipulation using a topology-protected guiding channel. (a) The proposed new system is based on a topological photonic structure (the gray substrate), which supports a topology-protected guiding mode. Both sphere 1 and sphere 2 (the red spheres) are resonantly repelled from the substrate. (b) When particle 1 resonantly interacts with the incident light, a large repulsive force F_{z1} is obtained. At the same time, the optical force F_{z2} on particle 2 is also large enough, because the topologically protected mode almost keeps its original form after the resonant interaction with sphere 1. This merit makes multiple and parallel resonant optical manipulation possible.

2. RESULTS AND DISCUSSION

A. Topological Photonic Slabs

As an illustration of example, here we use a honeycomb photonic crystal to achieve the topological photonic structures by deforming the honeycomb lattice [27]. Figure 3(a) shows the schematic of the topological photonic crystal structure, which is implemented on a GaAs dielectric substrate. We start from a honeycomb lattice with the hexagonal clusters composed of six neighboring equilateral triangular holes (white) with a side length of S. The black-dashed hexagons are primitive cells (with a lattice constant a_0) of the honeycomb, and the centroids of the triangular hole are located a_1 from the center of the cell. When $a_1{:}a_0 > 1{:}3$, we say the structure is an expanded lattice. On the contrary (i.e., $a_1{:}a_0 < 1{:}3$), it is named a shrunken lattice. It has been demonstrated that the expanded structure ($a_1{:}a_0 = 1.09{:}3$) produces a nontrivial band gap, while the shrunken structures ($a_1{:}a_0 = 0.91{:}3$) produce a trivial band gap [27–29].

Figure 3(b) shows the band structure of the TE modes along the x direction. Here, the structure is periodic along the x direction, and the thickness along the z axis is h. Along the y axis, there are 10 unit cells in both the shrunken and expanded regions. The band structure reveals the presence of two edge states crossing the band gap, indicating the existence of

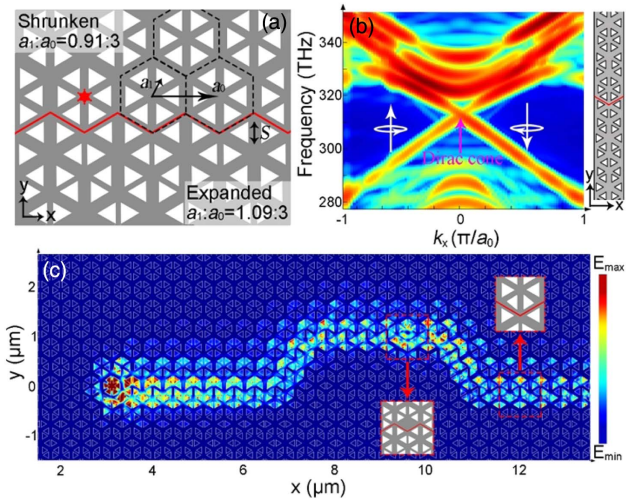

Fig. 3. Structure, parameter, and performance of the topologically protected guiding channel. (a) Schematic of the topological photonic structure composed of two different honeycomb lattices. a_0 is the lattice constant. S is the side lengths of the triangular holes (equilateral triangle). h is the thickness of the structure. a_1 is the relative position of the triangular hole to the center of the unit cell. When $a_1{:}a_0 > 1{:}3$, we say that the structure is expanded. On the contrary, it is a shrunken one. The parameters used are $a_0 = 445$ nm, $h = 0.2$ μm, $S = 140$ nm. (b) Corresponding band structure of the TE modes along the x direction (see the inset). Crossing of the two edge states in the band gap is the character of topologically protected edge states. The frequency of the crossing point is at about 315 THz. (c) Electric field distribution of the light propagation in the topological photonic structure at the frequency of 315 THz. Owing to the topology-protected feature, the propagation of the light field is immune to the local defects (red-dotted box) and sharp turns and can be perfectly transmitted without obvious loss or backscattering.

topologically protected edge states [25,26]. On the interface of the shrunken and expanded lattice structures, a topology-protected guiding channel is supported.

Using the three-dimensional finite difference time domain (FDTD) method, we get the propagation properties of light in the trapezoidal structure composed of expanded and shrunken structures, as shown in Fig. 3(c). The structure is excited by a circularly polarized electric dipole (at the frequency of 315 THz) located at the position marked in Fig. 3(a). The light propagation is strictly confined to the interface and can be perfectly transmitted without obvious loss or backscattering even through four cascade sharp turns. It is noted that the topological edge state is broadband and can maintain robust transmission from 300 to 323 THz.

B. Optical Force of Particles on the Topological Photonic Slabs

Now, let us quantitatively analyze the optical force on the particles when they are near the topological PC structure, as illustrated in Fig. 2(a). Without loss of generality, the particles are made of Si_3N_4 with a refractive index of $n = 2.0$. The time-averaged optical force F acting on the particle can be calculated by integrating Maxwell's stress tensor T over a closed surface surrounding it [8,30]:

$$F = \oint_S \langle T \rangle \cdot n \mathrm{d}S, \tag{1}$$

where $\langle \cdot \rangle$ means a temporal average, and n is the outward unit normal vector from the closed surface S.

The resonance condition is satisfied for a series of radii, which is known as morphology dependent resonances (MDRs) [30]. The MDR is related to the incident light frequency, and the resonance shifts when the light frequency changes. Since the optical force peak repeats periodically with the particle radius, only the values of F_x and F_z in one period are shown in Fig. 4(a). Similar to the traditional waveguide structure [see Fig. 1(c)], the optical forces on the first sphere in the topological structure also have peak values at the resonant radius. More importantly, the forces on the second sphere are only decreased moderately when compared to the cases in Fig. 1(c) due to the robust topologically protected feature of the structure, which greatly reduces the resonant loss of the guiding mode at the presence of the first sphere. Here the force comparison between the two structures is fair because all the parameters of the two structures are almost the same.

At the resonant point A marked in Fig. 4(a1), F_x on the first and second particles is 1.47 and 0.98 pN/mW, respectively. F_z on the first and second particles is 2.62 and 1.92 pN/mW [Fig. 4(a2)], respectively. The ratios of them are $F_{x2}/F_{x1} = 66.7\%$ and $F_{z2}/F_{z1} = 73.3\%$. On the contrary, for the case of the ordinary planar waveguide, the F_{x2}/F_{x1} and F_{z2}/F_{z1} are only about 13.9% and 18.7% at resonant conditions [see Fig. 1(d)]. This means that the topology-protected guiding mode can sort subsequent particles much more effectively than an ordinary surface wave. It is noted that the particles are all perfect spheres in simulation. Our results show that the sorting can also be carried out smoothly when the particles are slightly deformed, as long as the resonance condition is satisfied.

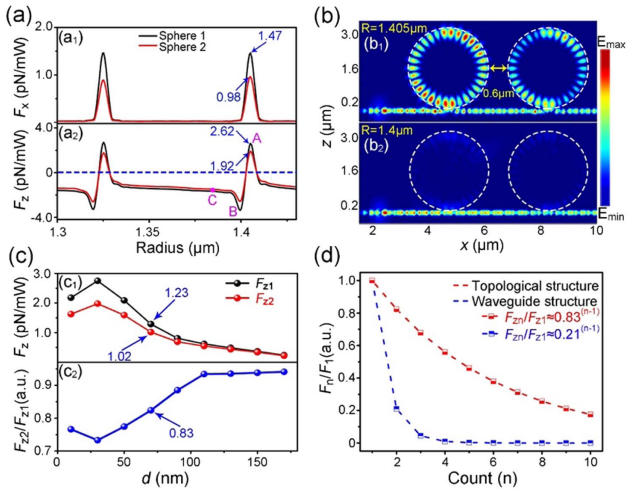

Fig. 4. Optical forces on two spheres using the topological structure designed in Fig. 2(a). (a) Optical forces F_x and F_z as functions of particle radius r at the source frequency of 315 THz. Comparing the forces on particle 1, the forces on particle 2 are decreased moderately only due to the topologically protected feature of the guiding channel. Note that the optical force repeats periodically with the radius, showing one period only here. The two particles are to be manipulated in water. (b) Cross section of the electric field distribution on the x–z plane when the two particles are trapped on the topological PC structure. The radii of the spheres in (b_1) and (b_2) correspond to the points A and B marked in (a). (c) Resonant optical force F_z on the two particles (upper part) and the ratio of F_{z2}/F_{z1} (lower part) at various distances d. (d) The ratios of optical forces on the nth particle to the first particle when ten particles are simultaneously manipulated on the topological (red curve) and ordinary (blue curve) waveguides. The curve decay rate represents the perturbation degree of the particles to the transmitted light.

Figure 4(b) shows the electric field distributions along the x–z cross section when two particles are trapped (with an edge-to-edge interval of 0.6 μm). The particles in the upper part (b_1) and lower part (b_2) correspond to the points A and B marked in Fig. 4(a), respectively. Results show that the light field was well-confined in the topological interface in both cases. Here, one can observe that the interaction between the two particles is negligible. Actually, even when two particles are close enough (such as the interval decreased to 40 nm or even smaller), the light field can still transmit stably due to the topology-protected feature. This ensures that the subsequent particles are subjected to a strong optical force robustly.

For the optical sorting of multiple particles, the distance d between the particle and the surface of the plate is crucial. The variation of d induces significant changes in the resonant force and the ratio F_{z2}/F_{z1}, as shown in Fig. 4(c). Here the radius of particle is at the resonance Point A marked in Fig. 4(a). Starting from a small value of $d = 10$ nm, the peak force increases with d, and the maximum force is obtained at $d = 30$ nm. Subsequently, the peak force decreases monotonously when $d > 30$ nm, while the ratio F_{z2}/F_{z1} increases gradually. This is mainly due to the coupling efficiency between the guiding channel and the particles, which has been discussed in Ref. [15]. When $d = 70$ nm, F_{z2} is 1.02 pN/mW, which

is 83% of that on the first particle. This ensures that the particles are subject to larger optical forces, and subsequent particles can still be manipulated efficiently.

In order to compare the multiparticle manipulation efficiencies of the topological and ordinary waveguide structures, 10 identical particles are introduced for illustration, and their ratios of F_{zn}/F_{z1} were shown in Fig. 4(d). Here, $n = 1, 2, \ldots, 10$ is the index of the particle. For an ordinary waveguide structure at $d = 70$ nm, the optical force of the third particle is already negligible ($F_{z3}/F_{z1} \approx 4.4\%$) under the resonance condition, which means that not more than two particles can be manipulated at the same time. In contrast, for the topological structure at $d = 70$ nm, the optical force on the 10th particle remains at a higher level ($F_{z10}/F_{z1} \approx 18.7\%$) under the resonance conditions due to the topology-protected guiding mode. This result indicates multiparticle optical sorting based on resonance enhanced optical forces is possible in a topological photonic structure.

C. Multiparticle Optical Sorting

From Fig. 4(a2), one can find that the sign of F_z is periodically dependent on the radius of the particles. Particles with some radii will be repelled by the topological PC structure, while others will be attracted to it. This provides a principle of optical sorting. For example, the particle with a radius from 1.329 to 1.401 μm will be attracted to the substrate. On the other hand, the particle with a radius from 1.402 to 1.408 μm will be pushed away from the slab. The dynamic characterization of the particles on the topological PC slab can be found by the temporal evolution of the particle motion equation, which will be discussed in detail in the following.

In a liquid environment, it should be noted that the particles are subjected to several other forces in addition to the optical force in the process of movement, including Brownian force, drag force, gravity, and buoyancy. For simplicity, the particles are placed in a static water environment, the drag force due to the flow of the liquid and the resistance provided by the shear flow are ignored [31,32], and only the drag force caused by the particles' movement is considered. In addition, the contributions of gravity ($\sim 10^{-13}$ N) and buoyancy ($\sim 10^{-13}$ N) are 1 order smaller in amplitude compared to other forces for the parameters used in this work [12,33–36]. Therefore, we can describe the motion of the particle in the following equations [34,37]:

$$m_p \ddot{s}(t) = F_{\text{opt}} - F_{\text{Br}} - F_d, \tag{2}$$

$$F_{\text{Br}} = R\sqrt{(12\pi k_B T r \eta)/\Delta t}, \tag{3}$$

$$F_d = 6\pi r \eta \dot{s}(t), \tag{4}$$

where the three main forces, i.e., optical force F_{opt}, Brownian force F_{Br}, and drag force F_d, are taken into account. m_p and r are the mass and radius of the particle, respectively; $s(t)$ is the particle's time-dependent position; k_B and T are the Boltzmann constant and the temperature in Kelvin; $\eta = 9.1 \times 10^{-4}$ Pa · s is the dynamic viscosity of water at room-temperature [38]; R is a Gaussian random number with a zero mean and standard deviation of 1; Δt is the time interval (we set Δt to be 10^{-4} s in order to get an accurate result); the F_{opt} is the optical force, which could be calculated by the Maxwell's stress tensor (MST) according to Eq. (1).

In order to analyze the feasibility of multiparticle resonant optical sorting in the topological photonic structure, three types of particles [corresponding to A, B, C marked in Fig. 4(a)] were mixed and placed randomly on the surface of the slab, as shown in Fig. 5(a). To understand the optical sorting along the z direction more clearly, one left-handed circularly polarized electric dipole and a right-handed one (with a light source power of 30 mW) are introduced, as shown by the red and blue asterisks. The two dipoles excite two counterpropagating topologically protected modes. In this case, the optical forces along the x axis will be balanced, and the force along the z axis is highlighted. For clarity, the position of the left electric dipole (red hexagon) is defined as the origin of the xyz coordinate system. In the simulation, the initial distance d between the particle and the slab is set to be 70 nm, where $F_{z2}/F_{z1} = 83\%$ as shown in Fig. 4(d1).

The time evolution dynamics of the particles on the topological photonic slab shown in Fig. 5(a) is numerically analyzed using the Eqs. (2)–(4). For the particles of type A (the red spheres), they experience repulsive forces in the z direction and are driven away from the slab. Their trajectories are shown in Fig. 5(b). Clearly, all of them are selected from the particle mixture. For type B and type C particles, since the total force in the z direction is always negative [Fig. 5(d)], particles are attracted to the slab.

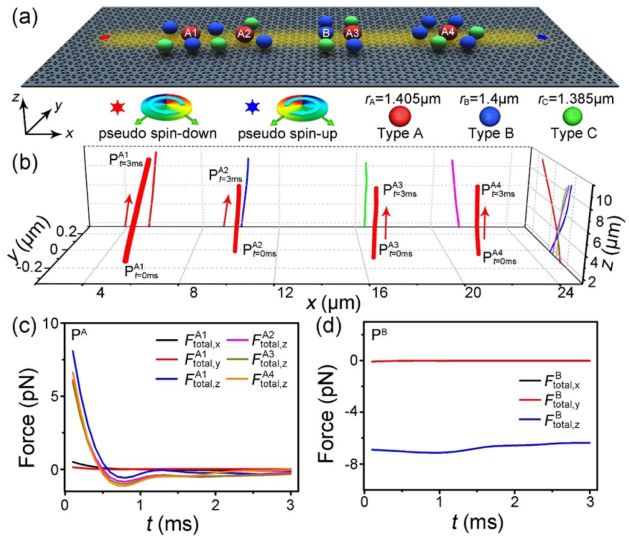

Fig. 5. Dynamics of the resonant multiparticle sorting using the topological photonic slab. (a) Schematic of multiparticle optical sorting scheme using the topological structure, where a mixture of the three types of particles A, B, C marked in Fig. 4(a2) is randomly placed on the surface of the substrate. (b) Trajectories of mass center of the four type A particles (A1, A2, A3, and A4) as a function of time. (c) Temporal evolution of total force on the type-A particles. The forces on all particles on the slab are calculated simultaneously. (d) Temporal evolution of the total force on the type B particle of P^B. It is noted that $F_{\text{total},x}$ and $F_{\text{total},y}$ are almost totally overlaped and both are nearly zero.

Taking the particle P^{A1} as an example, the temporal evolutions of the optical forces are shown in Fig. 5(c). In the z direction, the particle is first pushed away from the slab by a large force in the z direction, and then the force decreases and approaches zero as the particles move far away from the slab. In the x–y plane, the particles are almost stationary because the forces cancel each other out in the x and y directions for all the three types of particles.

From the trajectories of particles, it can be seen that the particles with the radius $r_{Fz<0}$ will be attracted while the particles with the radius $r_{Fz>0}$ will be repelled from the substrate. More importantly, by comparing the trajectories of the type A particles, it is found that the influence of other particles is very weak. When a large number of particles of a different radius pass through the surface of the topological PC slab, the particles resonant with the incident frequency will be repelled from the surface of the slab, while others will be trapped on the surface of the slab. By changing the frequency of the incident source, each type of particle can be sorted step by step using the similar method. Therefore, multiparticle optical sorting is achieved.

The proposed optical sorting scheme could be implemented in a topological PC structure, which can be fabricated by electron beam lithography [39]. By introducing quantum dots or a standard waveguide, the topological edge states with robustness and broad bandwidth operation can be guaranteed [40–42]. In particular, the optical guiding of submicrometer dielectric particles on the photonic crystal waveguides has been achieved experimentally in Ref. [43]. In short, the feasibility of optical sorting using a topological photonic structure and its application in the biological field are still open, which should motivate further research on this topic [44]. Further, combining it with microfluidic chips to build miniaturized and portable biochemical detection devices is also a possible direction of future research [45].

3. CONCLUSION

In conclusion, we have proposed a powerful optical sorting platform using a topological photonic structure, which supports a topology-protected optical mode immune to local disorders and the particles to be manipulated. Based on this merit, an efficient optical sorting scheme for multiple and parallel sorting is proposed and investigated numerically. This scheme offers several advantages. First, this sorting method is realized at resonance, which utilizes the laser power to enhance the optical force and improve the sorting efficiency. Second, it supports high throughput and parallel sorting manipulation, as the topological protection property ensures that a large number of resonant particles can be manipulated simultaneously. Last but not the least, the topological slab is well suited for integration with a lab-on-a-chip platform. Although only a pilot demonstration of this new optical sorting mechanism is performed, it paves the way for future experimental study of efficient optical sorting based on chip integration for biophysical and biochemical analysis.

Funding. National Natural Science Foundation of China (11874134, 12104083, 21973023); Fundamental Research Funds for the Central Universities (HIT.OCEF.2021020).

Disclosures. The authors declare no conflicts of interest.

Data Availability. Data underlying the results presented in this paper are not publicly available at this time but may be obtained from the authors upon reasonable request.

REFERENCES

1. J. M. Hou, M. G. Krebs, L. Lancashire, R. Sloane, A. Backen, R. K. Swain, L. J. C. Priest, A. Greystoke, C. Zhou, K. Morris, T. Ward, F. H. Blackhall, and C. Dive, "Clinical significance and molecular characteristics of circulating tumor cells and circulating tumor microemboli in patients with small-cell lung cancer," J. Clin. Oncol. **30**, 525–532 (2012).
2. M. M. Wang, E. Tu, D. E. Raymond, J. M. Yang, H. C. Zhang, N. Hagen, B. Dees, E. M. Mercer, A. H. Forster, I. Kariv, P. J. Marchand, and W. F. Butler, "Microfluidic sorting of mammalian cells by optical force switching," Nat. Biotechnol. **23**, 83–87 (2004).
3. N. M. Karabacak, P. S. Spuhler, F. Fachin, E. J. Lim, V. Pai, E. Ozkumur, J. M. Martel, N. Kojic, K. Smith, P. Chen, J. Yang, H. Hwang, B. Morgan, J. Trautwein, T. A. Barber, S. L. Stott, S. Maheswaran, R. Kapur, D. A. Haber, and M. Toner, "Microfluidic, marker-free isolation of circulating tumor cells from blood samples," Nat. Protoc. **9**, 694–710 (2014).
4. A. Atajanov, A. Zhbanov, and S. Yang, "Sorting and manipulation of biological cells and the prospects for using optical forces," Micro Nano Syst. Lett. **6**, 2 (2018).
5. A. H. J. Yang, S. D. Moore, B. S. Schmidt, M. Klug, M. Lipson, and D. Erickson, "Optical manipulation of nanoparticles and biomolecules in sub-wavelength slot waveguides," Nature **457**, 71–75 (2009).
6. R. W. Applegate, J. Squier, T. Vestad, J. Oakey, D. W. M. Marr, P. Bado, M. A. Dugand, and A. A. Said, "Microfluidic sorting system based on optical waveguide integration and diode laser bar trapping," Lab Chip **6**, 422–426 (2006).
7. H. Li, Y. Y. Cao, B. J. Shi, T. T. Zhu, Y. Geng, R. Feng, L. Wang, F. K. Sun, Y. Z. Shi, M. A. Miri, M. N. Vesperinas, C. W. Qiu, and W. Q. Ding, "Momentum-topology-induced optical pulling force," Phys. Rev. Lett. **124**, 143901 (2020).
8. H. Li, Y. Y. Cao, L. M. Zhou, X. H. Xu, T. T. Zhu, Y. Z. Shi, C. W. Qiu, and W. Q. Ding, "Optical pulling forces and their applications," Adv. Opt. Photon. **12**, 288–366 (2020).
9. T. T. Zhu, Y. Y. Cao, L. Wang, Z. Q. Nie, T. Cao, F. K. Sun, Z. H. Jiang, C. W. Qiu, and W. Q. Ding, "Self-induced backaction optical pulling force," Phys. Rev. Lett. **120**, 123901 (2018).
10. L. N. Ng, B. J. Luf, M. N. Zervas, and J. S. Wilkinson, "Forces on a Rayleigh particle in the cover region of a planar waveguide," J. Lightwave Technol. **18**, 388–400 (2000).
11. S. Gaugiran, S. Gétin, J. M. Fedeli, and J. Derouard, "Polarization and particle size dependence of radiative forces on small metallic particles in evanescent optical fields. Evidences for either repulsive or attractive gradient forces," Opt. Express **15**, 8146–8156 (2007).
12. L. N. Ng, B. J. Luff, M. N. Zervas, and J. S. Wilkinson, "Propulsion of gold nanoparticles on optical waveguides," Opt. Commun. **208**, 117–124 (2002).
13. S. Gaugiran, S. Gétin, J. M. Fedeli, G. Colas, A. Fuchs, F. Chatelain, and J. Dérouard, "Optical manipulation of microparticles and cells on silicon nitride waveguides," Opt. Express **13**, 6956–6963 (2005).
14. Y. Z. Shi, S. Xiong, L. K. Chin, J. B. Zhang, W. Ser, J. H. Wu, T. N. Chen, Z. C. Yang, Y. L. Hao, B. Liedberg, P. H. Yap, D. P. Tsai, C. W. Qiu, and A. Q. Liu, "Nanometer-precision linear sorting with synchronized optofluidic dual barriers," Sci. Adv. **4**, eaao0773 (2018).
15. Y. C. Li, O. V. Svitelskiy, A. V. Maslov, D. Carnegie, E. Rafailov, and V. N. Astratov, "Giant resonant light forces in microspherical photonics," Light Sci. Appl. **2**, e64 (2013).
16. S. Y. Lin, E. Schonbrun, and K. Crozier, "Optical manipulation with planar silicon microring resonators," Nano Lett. **10**, 2408–2411 (2010).
17. A. Einat and U. Levy, "Analysis of the optical force in the micro ring resonator," Opt. Express **19**, 20405–20419 (2011).

18. K. Grujica, O. G. Hellesø, J. S. Wilkinson, and J. P. Hole, "Optical propulsion of microspheres along a channel waveguide produced by Cs^+ ion-exchange in glass," Opt. Commun. **239**, 227–235 (2002).
19. B. S. Schmidt, A. H. J. Yang, D. Erickson, and M. Lipson, "Optofluidic trapping and transport on solid core waveguides within a microfluidic device," Opt. Express **15**, 14322–14334 (2007).
20. G. Brambilla, G. S. Murugan, J. S. Wilkinson, and D. J. Richardson, "Optical manipulation of microspheres along a subwavelength optical wire," Opt. Lett. **32**, 3041–3043 (2007).
21. R. F. Marchington, M. Mazilu, S. Kuriakose, V. Garcés-Chávez, P. J. Reece, T. F. Krauss, M. Gu, and K. Dholakia, "Optical deflection and sorting of microparticles in a near-field optical geometry," Opt. Express **16**, 3712–3726 (2008).
22. G. S. Wiederhecker, L. Chen, A. Gondarenko, and M. Lipson, "Controlling photonic structures using optical forces," Nature **462**, 633–636 (2009).
23. M. L. Povinelli, M. Loncar, M. I. Banescu, E. J. Smythe, and J. D. Joannopoulos, "Evanescent-wave bonding between optical waveguides," Opt. Lett. **30**, 3042–3044 (2005).
24. P. T. Rakich, M. A. Popović, M. Soljačić, and E. P. Ippen, "Trapping, corralling and spectral bonding of optical resonances through optically induced potentials," Nat. Photonics **1**, 658–665 (2007).
25. L. Lu, J. D. Joannopoulos, and M. Soljačić, "Topological photonics," Nat. Photonics **8**, 821–829 (2014).
26. A. B. Khanikaev and G. Shvets, "Two-dimensional topological photonics," Nat. Photonics **11**, 763–773 (2017).
27. S. Barik, H. Miyake, W. DeGottardi, E. Waks, and M. Hafezi, "Two-dimensionally confined topological edge states in photonic crystals," New J. Phys. **18**, 113013 (2016).
28. L. H. Wu and X. Hu, "Scheme for achieving a topological photonic crystal by using dielectric material," Phys. Rev. Lett. **114**, 223901 (2015).
29. X. D. Chen, X. T. He, and J. W. Dong, "All-dielectric layered photonic topological insulators," Laser Photon. Rev. **13**, 1900091 (2019).
30. H. Y. Jaising and O. G. Hellesø, "Radiation forces on a Mie particle in the evanescent field of an optical waveguide," Opt. Commun. **246**, 373–383 (2005).
31. G. P. Krishnan and D. T. Leighton, "Inertial lift on a moving sphere in contact with a plane wall in a shear flow," Phys. Fluids **7**, 2538–2545 (1995).
32. A. J. Goldman, R. G. Cox, and H. Brenner, "Slow viscous motion of a sphere parallel to a plane wall—II Couette flow," Chem. Eng. Sci. **22**, 653–660 (1967).
33. D. A. Shilkin, E. V. Lyubin, M. R. Shcherbakov, M. Lapine, and A. A. Fedyanin, "Directional optical sorting of silicon nanoparticles," ACS Photon. **4**, 2312–2319 (2017).
34. W. H. Xu, Y. Y. Wang, W. X. Jiao, F. Wang, X. F. Xu, M. Jiang, H. P. Ho, and G. H. Wang, "Tunable optofluidic sorting and manipulation on micro-ring resonators from a statistics perspective," Opt. Lett. **44**, 3226–3229 (2019).
35. L. Wang, Y. Y. Cao, B. J. Shi, H. Li, R. Feng, F. K. Sun, L. Y. Lin, and W. Q. Ding, "Subwavelength optical trapping and transporting using Bloch mode," Opt. Lett. **45**, 1886–1889 (2020).
36. Y. Z. Shi, S. Xiong, Y. Zhang, L. K. Chin, Y. Y. Chen, J. B. Zhang, T. H. Zhang, W. Ser, A. Larrson, S. H. Lim, J. H. Wu, T. N. Chen, Z. C. Yang, Y. L. Hao, B. Liedberg, P. H. Yap, K. Wang, D. P. Tsai, C. W. Qiu, and A. Q. Liu, "Sculpting nanoparticle dynamics for single-bacteria-level screening and direct binding-efficiency measurement," Nat. Commun. **9**, 815 (2018).
37. E. E. Michaelides, "Brownian movement and thermophoresis of nanoparticles in liquids," Int. J. Heat Mass Transfer **81**, 179–187 (2015).
38. Y. Zhang and B. J. Li, "Particle sorting using a subwavelength optical fiber," Laser Photon. Rev. **7**, 289–296 (2013).
39. C. P. Reardon, I. H. Rey, K. Welna, L. O'Faolain, and T. F. Krauss, "Fabrication and characterization of photonic crystal slow light waveguides and cavities," J.Vis. Exp. **69**, e50216 (2012).
40. S. Barik, A. Karasahin, C. Flower, T. Cai, H. Miyake, W. DeGottardi, M. Hafezi, and E. Waks, "A topological quantum optics interface," Science **359**, 666–668 (2018).
41. X. T. He, E. T. Liang, J. J. Yuan, H. Y. Qiu, X. D. Chen, F. L. Zhao, and J. W. Dong, "A silicon-on-insulator slab for topological valley transport," Nat. Commun. **10**, 872 (2019).
42. M. I. Shalaev, W. Walasik, A. Tsukernik, Y. Xu, and N. M. Litchinitser, "Robust topologically protected transport in photonic crystals at telecommunication wavelengths," Nat. Nanotechnol. **14**, 31–34 (2019).
43. M. G. Scullion, Y. Arita, T. F. Krauss, and K. Dholakia, "Enhancement of optical forces using slow light in a photonic crystal waveguide," Optica **2**, 816–821 (2015).
44. M. Jung, R. G. Gladstone, and G. Shvets, "Nanopolaritonic second-order topological insulator based on graphene plasmons," Adv. Photon. **2**, 046003 (2020).
45. Y. J. Yang, Y. X. Ren, M. Z. Chen, Y. Arita, and C. R. Guzmán, "Optical trapping with structured light: a review," Adv. Photon. **3**, 034001 (2021).